Research Square

Preprints are preliminary reports that have not undergone peer review.
They should not be considered conclusive, used to inform clinical practice,
or referenced by the media as validated information.

Morphology-dependent efficacy of Chlorella vulgaris biostimulants in alleviating salinity stress in rice

Jia-Jia Zhang
Hexi University
Yue-Ying Liu
Hexi University
Hai-Yan Liu
Hexi University
Guang-Hong Luo
Hexi University
Liang Yin
yinl03@163.com
Hexi University

Research Article

Keywords: Microalgal biofertilizer, immobilized algal beads, salt stress, rice, antioxidant enzymes, photosynthetic electron transport

Posted Date: September 7th, 2026

DOI: https://doi.org/10.21203/rs.3.rs-10799538/v1

License: This work is licensed under a Creative Commons Attribution 4.0 International License.
Read Full License

Additional Declarations: No competing interests reported.

Abstract

Salinity represents a major abiotic barrier to rice production. Microalgal biostimulants offer eco-friendly relief from salt stress, yet systematic comparisons across different algal formulations are still lacking. This study evaluated three formulations of the microalga *Chlorella vulgaris*: powder, paste, and immobilized sodium alginate–polyvinyl alcohol (SA–PVA) beads, on rice growth under 50 mM NaCl stress. Salinity significantly inhibited the growth, pigment content, and photosynthesis of untreated plants. However, all formulations alleviated salt-induced damage, with efficacy ranked as follows: immobilized beads > paste > powder. Notably, the immobilized beads treatment not only reversed growth inhibition but also outperformed the non-stressed control, restoring total chlorophyll levels to 134.9% of the control and reducing malondialdehyde accumulation by 66.9% compared to salt-stressed seedlings. Furthermore, plants treated with immobilized algal beads under salinity stress exhibited a 200% increase in catalase (CAT) and a 63.5% increase in peroxidase (POD) activities, alongside a 52.2% reduction in superoxide dismutase (SOD) activity, indicating a synergistic shift from stress-induced redox imbalance to efficient reactive oxygen species (ROS) elimination. Mechanistically, the SA–PVA matrix established a rhizospheric barrier through Na^+ adsorption and extracellular polymeric substance (EPS)-mediated chelation. In addition, it enhanced the antioxidant cascade by upregulating CAT and POD, restoring SOD homeostasis, and preserving thylakoid electron transport by eliminating the OJIP K-band. These results establish formulation morphology as a critical determinant of biostimulant efficacy and highlight the potential of immobilized microalgae as a clean, sustainable biostimulant depot for crop protection in soilless cultivation systems.

Introduction

In recent years, global warming, environmental degradation, advances in controlled-environment agriculture, and improper irrigation practices have significantly exacerbated soil salinization (Tang et al. 2024). Furthermore, salt stress exerts the combined effects of osmotic stress and ion toxicity, leading to ionic imbalances and water deficiency within plant tissues. These conditions severely compromise the integrity of the plant cell membrane system, inhibit photosynthesis, impair plant growth, and ultimately cause plant death, thereby threatening the sustainability and productivity of regional agriculture (Arif et al. 2020; Banik et al. 2023).

Various strategies, including agronomic practices, molecular breeding, and gene-editing technologies, have been developed to alleviate salinity stress (Li et al. 2026; Nurbekova et al. 2024). However, these approaches are often time-consuming, labor-intensive, and costly, and their large-scale implementation remains challenging (Szabados et al. 2026; Yuan et al. 2025). Consequently, there is an urgent need to develop efficient, sustainable, and cost-effective strategies for maintaining crop productivity under adverse environmental conditions. The application of beneficial microorganisms, particularly salt-tolerant microalgae, has emerged as a promising, environmentally friendly strategy (Ali et al. 2022). Microalgae are rich in extracellular polysaccharides (EPS), phytohormones, vitamins, and other bioactive metabolites, which can enhance nutrient availability, regulate plant physiological processes, and activate

stress-signaling pathways (Sarsekeyeva et al. 2024; Sun et al. 2026), thereby enhancing seed germination, root development, and overall plant vigor (Herrera et al. 2025; Ouzakar et al. 2025). Moreover, EPS produced by cyanobacteria exhibit a remarkable capacity to chelate cations, thereby reducing Na^+ bioavailability, mitigating sodium ion toxicity, and improving the rhizospheric microenvironment under saline conditions (Arora et al. 2010; Durairaj et al. 2026).

Recent studies have demonstrated the potential of microalgae function as biostimulants to mitigate salinity-induced stress. For instance, Zhang et al. (2025) reported enhanced salinity tolerance in rice following cyanobacterial application. Nisha et al. (2018) observed that the application of the cyanobacteria *Nostoc ellipsosporum* and *Nostoc punctiforme* facilitated salt removal and significantly enhanced the growth and yield of wheat and pearl millet crops. Similarly, seed priming and inoculation with *Nostoc sp.* and *Anabaena doliolum* alleviated the detrimental effects of salinity in rice by limiting Na^+ ion uptake and reducing the accumulation of malondialdehyde (MDA) and superoxide radicals (Paul et al. 2026). Nogueira et al. (2025) further demonstrated that freshwater algal inoculation enhanced plant resilience to saline stress and increased productivity in two onion cultivars.

Microalgae-based biofertilizers, similar to chemical fertilizers, function as biostimulants and stress ameliorants and are available in various forms, including fresh algal suspensions or paste (algal paste), dried algal powder (algal powder), and immobilized algae, each exhibiting distinct characteristics and agronomic potential (Patel et al. 2025). However, comparative studies evaluating the efficacy of different morphological formulations of microalgal biostimulants on growth, pigment content, photosynthetic activity, and antioxidant enzyme activity under salinity stress remain scarce, particularly in rice. Therefore, this study aimed to evaluate the comparative effects of three morphological forms of microalgal biofertilizers on rice plants subjected to salinity stress.

Materials and methods

Development and formulation of biostimulants derived from microalgae

The eukaryotic microalgal strain *Chlorella vulgaris* was obtained from the Freshwater Algae Culture Collection at the Institute of Hydrobiology (FACHB), Chinese Academy of Sciences, Wuhan, China. The strain was cultured in BG-11 medium under a 12:12 h light: dark cycle at 25 ± 2°C with a light intensity of 72 µmol photons $m^{-2} \cdot s^{-1}$ (Rippka et al. 1979). The cells were harvested by centrifugation during the exponential phase of growth. To prepare the algal paste, the cells were collected by centrifugation, washed two to three times with distilled water, and centrifuged again to obtain fresh biomass. To prepare algal powder, the algal paste was dried at 80°C for 10 hours and subsequently ground into a fine powder. To prepare the immobilized algal beads, 3 g of sodium alginate (SA) and 9 g of polyvinyl alcohol (PVA) were dissolved in 150 mL of distilled water at 80°C. After cooling to 40°C, this mixture was combined with 3 g of fresh algal biomass and extruded dropwise into a 2% (w/v) $CaCl_2$ solution to form approximately 2-mm-diameter gel beads. The three formulations used in this study are shown in Fig. 1.

Rice cultivation and experimental design

Rice (*Oryza sativa* L. cv. White Awn) seeds provided by the Zhangye Academy of Agricultural Sciences were used. The seeds were surface-sterilized with 1% NaClO for 30 minutes, thoroughly rinsed with distilled water, and germinated in the dark at 30°C for 24 hours. Uniform seedlings were then transferred to hydroponic containers. The growth chamber conditions were maintained under a 12 h light/12 h dark photoperiod, a light intensity of 12,000 lx, day/night temperatures of 30 ± 2°C and 25 ± 2°C, respectively, and a relative humidity of approximately 80%.

The experiment was conducted using a completely randomized design with three replications. Salt stress was induced by supplementing the nutrient solution with 50 mM NaCl. The experimental treatments are listed in Table 1. After 14 days of treatment, the samples were collected for subsequent analyses.

Table 1. Experimental design showing the treatment groups

Treatments	Nomenclature
CK	0 mM NaCl
T0	50 mM NaCl
T1	50 mM NaCl + 1g/L algal powder
T2	50 mM NaCl + 1g/L algal paste
T3	50 mM NaCl + 1g/L immobilized algae beads

All treatments were applied hydroponically under controlled environmental conditions (28 **±** 2°C, 12 h light/12 h dark photoperiod, and a light intensity of 12,000 lx) for 14 days.

Analytical methods

Morphological indicators

Plant height and root length were measured using a ruler. Fresh weight (FW) was recorded immediately. In contrast, dry weight (DW) was determined after drying the samples at 105°C for 30 minutes to terminate enzymatic activity, followed by drying at 80°C to a constant weight.

Root morphological analysis

For morphological analysis, root systems were scanned at 300 dpi using a dual-light source flatbed scanner (Epson Perfection V700 Photo, Epson, Japan). The resulting images were processed using WinRHIZO Pro 2013 software (Regent Instruments Inc., Canada). The software automatically quantified the following root traits: total root length (cm), total root surface area (cm^2), average root diameter (mm), total root volume (cm^3), number of root tips, and number of forks.

Physiological assays

Chlorophyll content and antioxidant enzyme activity were assessed using fully expanded leaves and intact root systems collected from seedling-stage plants. Chlorophyll content was determined following extraction using an acetone–ethanol mixture. Catalase (CAT) activity was measured using a CAT activity detection kit, peroxidase (POD) activity was measured using a POD activity detection kit, and superoxide dismutase (SOD) activity was measured using a total SOD activity detection kit based on the nitroblue tetrazolium method **(Spitz et al.** 1989). MDA content was determined using an MDA detection kit based on the thiobarbituric acid colorimetric method (Heath et al. 1968). All kits were procured from Beijing Solarbio Biotechnology Co. Ltd.

Chlorophyll fluorescence

Dark-adapted leaves (20 min) were analyzed using a pulse-amplitude-modulated fluorometer. The OJIP transient was recorded under saturating red light at an intensity of 3,000 μmol $m^{-2} \cdot s^{-1}$. The key parameters analyzed included the photochemical quenching coefficient, non-photochemical quenching, and the maximum photochemical efficiency of PSII (Fv/Fm, where Fv = Fm − Fo). Each leaf was measured three times, and the original OJIP transient data were exported immediately after their acquisition.

Statistical analysis

Data were compiled and statistically analyzed using SPSS version 26.0. The results are presented as the mean ± standard deviation of three replicates. Statistical significance was determined using one-way analysis of variance at $P < 0.05$ under a completely randomized design.

Results

Plant growth and biomass measurements

Under 50 mM NaCl stress, rice growth was significantly inhibited. The phenotypic differences among treatments can be visually observed in Fig. 2, and the quantitative data for plant height and root length are summarized in Table 2. Compared with that of the control (CK), the plant height in the T0 group decreased by 61.1%. However, algal treatments significantly alleviated salt-induced growth inhibition. T3 treatment (immobilized beads) showed the greatest recovery, with plant height surpassing that of the CK. Specifically, the plant height in T3 was 234.3% higher than that in T0. Root growth was even more sensitive to salinity stress, with the root length in T0 reaching only 12.0% of the CK value. After algal application, root lengths in T1, T2, and T3 reached 25.5%, 38.7%, and 85.1% of the CK level, respectively. Notably, the T3 group exhibited a 611.9% increase in root length compared with that of T0. These findings suggest that the incorporation of microalgae bio-fertilizer formulations can effectively mitigate the suppressive effect of salt stress on the growth of stems and roots in rice seedlings.

Table 2
Plant height and root length of *O. sativa* L. cv. White Awn seedlings under different microalgal biostimulants treatments after 14 days of salt stress

Treatments	Plant height/cm	Root length/cm
CK	18.00 ± 0.9^{b}	14.80 ± 1.2^{a}
T0	7.00 ± 0.2^{d}	1.77 ± 0.3^{e}
T1	8.67 ± 0.8^{d}	3.77 ± 0.3^{d}
T2	11.90 ± 0.6^{c}	5.73 ± 0.4^{c}
T3	23.40 ± 2.0^{a}	12.60 ± 1.0^{b}

CK: distilled water without NaCl; T0: 50 mM NaCl stress only; T1: 50 mM NaCl + 1 $g \cdot L^{-1}$ algae powder; T2: 50 mM NaCl + 1 $g \cdot L^{-1}$ algae paste; T3:50 mM NaCl + 1 $g \cdot L^{-1}$ immobilized algal beads. Values are presented as mean ± standard error (n = 3). Different lowercase letters within the same column indicate significant differences among treatments at $P < 0.05$ (Duncan's multiple range test).

Biomass accumulation followed a similar trend (Fig. 3). Salt stress reduced FW and DW in T0 by 49.3% and 51%, respectively. T3 treatment not only restored biomass to CK levels but also exceeded them, with FW reaching 137.9% of that of the CK treatment. This “super-recovery” effect was most pronounced in the immobilized algal bead treatment group.

Figure 4 shows the root scanning images and various root parameters for each treatment group under salt stress conditions. The results revealed a significant decrease in all root parameters in the T0 group following salt stress, with the root surface area and bifurcation number exhibiting the most pronounced reductions. The subsequent application of different microalgal fertilizers significantly enhanced root growth across all treatment groups. Salt stress severely inhibited root system development, causing a substantial decline in the total number of roots and bifurcations in the T0 group, which were only 10.5% and 9.6% of those in the CK group, respectively. This decline indicates a strong inhibitory effect of salt stress on lateral root formation and elongation. Additionally, the total root length and surface area were significantly reduced, reaching only 27.5% and 26.4% of the corresponding values in the CK group, respectively. The increase in the average root diameter was also impeded, and the root cells exhibited expansion rather than elongation. In contrast, T3 treatment significantly promoted root system development, with the total root number and bifurcations reaching 1.69- and 1.71-fold higher than those of the CK group, respectively. Although the average root diameter in T3 was slightly reduced, the substantial increase in root length and branching suggests the formation of a highly efficient root architecture for nutrient and water uptake under stress conditions. Although algal paste and powder treatments showed promotive effects, the increase in root system parameters was considerably lower than that observed with immobilized algal beads.

Chlorophyll and photosynthesis assessment

Chlorophyll, the primary component of the light-harvesting antenna complex, is essential for maintaining the stability of photosynthetic processes and plant tolerance to environmental stress. As shown in Fig. 5, After 14 days of salt stress treatment, the chlorophyll a content in the CK group was 1.628 $mg \cdot g^{-1}$, whereas that in the T0 group decreased to 0.760 $mg \cdot g^{-1}$, representing a 53.3% decline, highlighting the detrimental impact of salt stress on the rice photosynthetic system. After the application of algal fertilizer, the chlorophyll a content in groups T2 and T3 increased to 2.142 and 2.196 $mg \cdot g^{-1}$, respectively, representing increases of 281.8% and 288.9% relative to group T0, and both were significantly higher than those observed in group T1. Regarding chlorophyll b content, group T0 exhibited a value of 0.461 $mg \cdot g^{-1}$, which was 18.55% lower than that of CK (0.566 $mg \cdot g^{-1}$). The highest content was observed in group T3 (0.929 $mg \cdot g^{-1}$), significantly surpassing that observed in the other groups. The fluctuation in total chlorophyll content mirrored that of chlorophyll a, decreasing from 2.194 $mg \cdot g^{-1}$ in the CK group to 1.221 $mg \cdot g^{-1}$ in the T0 group, representing a 44.3% decrease in the latter. After algal fertilizer application, the most substantial enhancement was observed in group T3, which exhibited a 255.9% increase compared with T0, surpassing the improvements observed in T1 and T2. In summary, salt stress substantially reduced chlorophyll accumulation, indicating impairment of the photosynthetic machinery. All three algal fertilizer formulations enhanced chlorophyll content and stress tolerance, with the immobilized algal beads in the T3 treatment showing the most favorable results. These results highlight the role of algal fertilizers in enhancing chlorophyll synthesis and its stability.

Fv/Fm is a key parameter for assessing the extent of photoinhibition and intrinsic photosynthetic capacity of plants. Figure 6 (A) shows that under 50 mM NaCl stress, the Fv/Fm value of the T0 treatment group was 0.549, representing a 13.7% reduction compared with the CK. This indicates significant damage to the PSII reaction center caused by salt stress, with severe impairment of the photosynthetic system. Upon the addition of various forms of microalgae fertilizers, Fv/Fm increased significantly in all T1, T2, and T3 treatment groups, surpassing that of the CK group.

The OJIP fluorescence kinetics curve (Fig. 6B) further revealed that, compared with the smooth ascending trajectory of the CK group, the T0 group exhibited a pronounced K-phase. Specifically, there was a significant increase in fluorescence at point J (approximately 2 ms), a slower rise at point I (approximately 30 ms), and a decrease in the maximum fluorescence at point P. These findings suggest that salt stress not only impairs the oxygen-evolving complex (OEC) but also hinders electron transfer from QA to QB and reduces the plastoquinone pool, resulting in multiple functional deficiencies on both the donor and acceptor sides of PSII.

The mitigating effects of the different microalgal fertilizer formulations were found to vary. The immobilized algal bead treatment shifted the overall curve downward, eliminated the K phase, and caused the J point to return, indicating superior OEC protection and improved electron transport efficiency. In the algal paste group, point I remained concave, suggesting a continued limitation of

plastoquinone pool reduction. The effect of algal powder treatment was comparatively modest, consistent with previous findings on antioxidants.

Antioxidant enzyme activity and MDA

The alterations in antioxidant enzyme activities and MDA accumulation triggered by saline exposure are summarized in Fig. 7. Under 50 mM NaCl stress, the activities of CAT and POD in rice seedlings were significantly inhibited, decreasing from 33.66 $U \cdot g^{-1}$ and 638.66 $U \cdot g^{-1}$ in the CK group to 12.24 $U \cdot g^{-1}$ and 323.17 $U \cdot g^{-1}$, respectively, representing reductions of 63.6% and 49.4%, respectively(Fig. 7A,B). This suggests that salt stress may impair antioxidant enzyme function, thereby diminishing the ability of these enzymes to eliminate reactive oxygen species. After the application of various algal fertilizers (algal powder T1, algal paste T2, and immobilized algal beads T3), the activities of both enzymes gradually recovered, with the restoration effect showing a clear dependence on the fertilizer form (T3 > T2 > T1). In particular, treatment with immobilized algal beads (T3) yielded the most favorable outcomes, with CAT activity rebounding to 36.72 $U \cdot g^{-1}$ (109.1% of the CK) and POD activity increasing to 885.33 $U \cdot g^{-1}$ (27.9% higher than CK). This not only completely reversed the inhibitory effect of salt stress but also significantly enhanced antioxidant capacity. The differences among the treatment groups were statistically significant ($P < 0.05$).

However, under 50 mM NaCl stress, SOD exhibited a contrasting response. SOD activity in rice seedlings increased sharply from 143.67 $U \cdot g^{-1}$ in the CK group to 489.33 $U \cdot g^{-1}$, representing a 240.6% increase ($P < 0.05$) (Fig. 7C). This indicates that salt stress triggers a substantial accumulation of $O_2^{-}\cdot$, prompting plants to activate the first line of antioxidant defense to convert $O_2^{-}\cdot$ into H_2O_2. After the application of various algal fertilizers (algal powder T1, algal paste T2, and immobilized algal beads T3), SOD activity exhibited a graded decline, with the degree of recovery showing a clear dependence on the form of fertilizer used (T3 > T2 > T1). In particular, treatment with immobilized algal beads (T3) demonstrated the most favorable outcome, as SOD activity decreased to 234.00 $U \cdot g^{-1}$, representing a 52.2% reduction compared with the T0 group, and rebounded to 61.4% of the CK level. This improvement was significantly greater than that observed in T1 (30.0% decrease) and T2 (36.5% decrease), with all differences among the treatment groups being significant.

After 14 days of exposure to 50 mM NaCl stress, the MDA content in the leaves of rice seedlings increased significantly from 4.700 $\mu mol \cdot g^{-1}$ in the CK group to 16.267 $\mu mol \cdot g^{-1}$, representing a 246.1% increase ($P < 0.05$) (Fig. 7D). This increase indicates that salt stress induces substantial lipid peroxidation damage to the membrane. After the application of various forms of algal fertilizers, MDA accumulation showed a gradient of inhibition, with the alleviation effect demonstrating a clear dependence on fertilizer formulation (T3 > T2 > T1). Specifically, the MDA content in groups T1, T2, and T3 decreased to 11.485, 6.122, and 5.382 $\mu mol \cdot g^{-1}$, respectively, corresponding to reductions of 29.4%, 62.4%, and 66.9% compared with that in group T0. Notably, the MDA content in the T3 group was only 14.5% higher than that in the CK group, and this difference was not statistically significant. These results

suggest that the immobilized algal beads nearly completely preserved cell membrane integrity, demonstrating significantly superior protective effects compared with algal powder and paste.

Discussion

This study comparatively evaluated the physiological recovery-promoting effects of algal powder, paste, and immobilized beads on rice seedlings subjected to salinity stress. Salt stress triggers a cascade of metabolic disturbances, oxidative stress, and ionic toxicity, which collectively constrain plant growth and development (Körner et al. 2025; Brito-Lopez et al. 2025). Microalgae-based biostimulants offer a promising and sustainable solution for enhancing agricultural practices (Brito-Lopez et al. 2025). The adverse effects of salinity stress on plants can be mitigated by applying *C. vulgaris* biofertilizer. The application of the three microalgal formulations consistently alleviated salt-induced growth inhibition, with the restorative efficacy ranked as follows: immobilized algal beads (T3) > algal paste (T2) > algal powder (T1).

Notably, plants treated with T3 not only completely overcame salinity-induced growth suppression but also surpassed CK levels, achieving plant height and root length greater than those of the non-stressed CKs and restoring total chlorophyll content to 134.9% of the CK value. Furthermore, MDA content in the T3 group was reduced to 14.5% above the CK level, indicating remarkable alleviation of membrane lipid peroxidation, with the extent of recovery significantly higher than that observed in the T1 and T2 treatments. These findings align with those of Zhang et al. (2025), who reported that the co-application of nitrogen-fixing cyanobacteria reduced rice MDA content by 40.01% while concurrently enhancing POD and CAT activities. Similarly, Senousy et al. (2023) reported that extracts of *C. vulgaris* and *Dunaliella salina* effectively reversed salinity-induced biomass decline in common beans (*Phaseolus vulgaris* L.).

The differential efficacy of the three formulations fundamentally arises from the influence of their physical morphologies on the preservation and delivery of bioactive compounds. In the case of algae powder (T1), drying at 80°C may have compromised thermolabile bioactive constituents, including exopolysaccharides and phytohormones, resulting in marked attenuation of its biostimulant activity (Arad S 2008; Stirk et al. 2021). Algae paste (T2), while retaining partial cellular integrity and bioactive components, lacks carrier-mediated protection, rendering free-living algal cells susceptible to rapid senescence under environmental fluctuations (Bailliez et al. 1986; Antara et al. 2024). In contrast, immobilized algal beads (T3) exploit the three-dimensional network of SA-PVA composites to create a stable microecological niche, enabling sustained and slow-release delivery of bioactive substances **(**Liang et al. 2022; Sarhan et al. 2024). The alginate gel matrix physically entraps microalgal cells within gel beads, and immobilization technology has been demonstrated to significantly enhance algal salt tolerance and prolong cell viability. Wang et al. (2024) reported that SA immobilization increases the growth rate of *C. vulgaris* by 50.7% under saline conditions while restoring photosynthetic electron transport activity. Similarly, Escalante et al. (2015) observed that the co-immobilization of *C. vulgaris* with plant growth-promoting bacteria significantly improved salt stress tolerance in tomato seedlings.

This structural advantage translated directly into physiological outcomes: in the T3 group, CAT activity increased from 12.24 to 36.72 U·g⁻¹, surpassing the CK level, whereas POD activity increased by 63.5% compared with that in T0. In contrast, the T1 and T2 groups achieved only limited physiological restoration, with CAT activity recovering to 36.4% and 63.6% of CK, respectively, which may be insufficient to normalize H_2O_2 metabolic flux. This suggests that their antioxidant defense systems remained in the stress acclimation phase rather than transitioning to a homeostatic reconstitution state.

The salinity-ameliorative effects of immobilized algal beads can be conceptualized as three tightly coupled hierarchically organized layers of activity. At the foundational level, physicochemical barriers exist within the rhizosphere. The porous architecture of SA-PVA gel beads facilitates the physical adsorption of free Na^+ ions, whereas microalgal EPS exhibits a strong affinity for cation binding and chelation. This dual-barrier mechanism may help limit Na^+ uptake by roots (Arora et al. 2010; Durairaj et al. 2026). Empirical evidence supporting this mechanism was observed in the T3 group, which showed a root length reaching 85.1% of the CK value and a 1.71-fold increase in the number of root branches. Building on this physical protection, the second tier involves the synergistic reprogramming of the antioxidant enzyme system.

The distinct antioxidant response observed in the T0 group, characterized by an increase in SOD activity alongside suppressed CAT and POD activities, suggests an imbalance in the ascorbate-glutathione cycle. The excessive accumulation of O_2^- likely overwhelms the downstream scavenging capacity, leading to H_2O_2 accumulation and subsequent membrane damage. Conversely, T3 treatment restored enzymatic homeostasis. The significant reduction in SOD activity in the T3 group indicates a lower generation rate of superoxide radicals, likely due to improved protection of the photosynthetic electron transport chain. Simultaneously, the upregulation of CAT and POD ensured the efficient detoxification of residual H_2O_2, thereby preventing lipid peroxidation. This interpretation is supported by the findings of Mutale-Joan et al. (2021), who reported that microalgal biostimulants promote plant growth under salinity stress via enhanced antioxidant activity. Mutale-Joan et al. (2021) and Wang et al. (2024) demonstrated that immobilized co-culture systems elevate EPS polysaccharide secretion by 19.7% under salt stress, with an increased proportion of aromatic proteins contributing to the enhanced structural stability. Ultimately, these two antecedent layers converge in the third tier: protection of the photosynthetic core machinery. The emergence of a K-band and elevation of the J-point in the OJIP transient of T0 plants denote, respectively, the impairment of the OEC and restriction of electron transfer from Q_A to Q_B. Upon algal bead treatment, the disappearance of the K-band and depression of the J-point indicate that immobilized beads may indirectly protect OEC integrity by attenuating rhizospheric Na^+ concentrations and preserve the functional integrity of the thylakoid membrane electron transport chain via enhancement of the antioxidative system, thereby ensuring the efficient operation of PSII reaction centers. This mechanistic hierarchy fundamentally underpins the remarkable recovery of chlorophyll a to 134.9% of the CK and the recovery of Fv/Fm beyond CK levels in the T3 group, demonstrating that the tripartite integration of physicochemical exclusion, enzymatic network

reprogramming, and photochemical core protection operates in a mutually reinforcing cascade rather than as an isolated mechanism.

Superior to algal powder and paste, SA–PVA immobilized beads act as self-replenishing biostimulant reservoirs tailored for commercial soilless cultivation. Hydroponics delivers an interference-free rhizosphere that enables sustained local release of phytohormones, EPS, and stress-signaling molecules from the composite matrix. The 1.71-fold elevation in root bifurcation relative to unstressed CK greatly improves rhizospheric nutrient acquisition. Beyond root architectural improvement, these beads function as biostimulants rather than conventional fertilizers to induce stable stress priming: suppressed SOD alongside elevated CAT and POD collectively redirect cellular metabolism toward energy-efficient redox homeostasis, conferring systemic salinity tolerance to recirculating nutrient solutions. Supported by dual rhizospheric Na^+ sequestration and photosystem protection effects verified in this study, the immobilized beads serve as a sustainable replacement for synthetic salinity regulators and facilitate brackish water reuse within closed protected agricultural systems. Collectively, their dual merits of boosted nutrient uptake and robust salt stress resistance confirm strong industrial potential for hydroponic production, yet further bead formulation optimization is required to extend efficacy to field soils

Although current hydroponic studies provide foundational proof of concept for the salinity-ameliorative efficacy of immobilized algal beads, extrapolation to field conditions must consider pedospheric complexities, including mechanical shearing, microbial colonization, and hydraulic flushing, which may collectively compromise gel integrity and alter the release kinetics (Castro et al. 2025; Benítez et al. 2025; Dey et al. 2011). The degradation dynamics of the SA-PVA matrix, encapsulated cell viability, and release dynamics of bioactive compounds in submergence-prone paddy systems remain critical knowledge gaps that require rigorous field-based investigations before the translational potential of this technology can be fully evaluated. Future studies will focus on field validation and transcriptomic profiling to elucidate the molecular mechanisms underlying the observed protective effects

Conclusion

This study demonstrates that formulation morphology critically determines the salinity-ameliorative efficacy of *C. vulgaris* biostimulants. The SA–PVA immobilized beads outperformed powder and paste formulations by establishing a rhizospheric Na^+ barrier, synergistically reprogramming the CAT–POD–SOD antioxidant network, and preserving thylakoid electron transport, thereby achieving superior growth recovery and photosynthetic protection. These findings establish immobilized microalgae as a promising bio-based strategy for sustainable crop production under saline conditions and warrant field validation to assess translational potential.

Declarations

Funding. This study was funded by Special Science and Technology Program of Ganzhou District (GZ2025JSNY02).

Competing interests. The authors declare no competing interests.

Availability of data and material. The data are available by request from the corresponding author.

Code availability. Not applicable

Author contributions Jia-Jia Zhang: Writing-original draft, Conceptualization, Data curation. Hai-Yan Liu: Writing—review & editing. Yue-Ying Liu: Methodology, Software. Guang-Hong Luo: Supervision, Validation. Liang Yin: Project design.

References

1. Ali Q, Ayaz M, Mu G, Hussain A, Yuanyuan Q, Yu C, Xu Y, Manghwar H, Gu Q, Wu H, Gao X (2022) Revealing plant growth-promoting mechanisms of Bacillus strains in elevating rice growth and its interaction with salt stress. *Frontiers in Plant Science* 13:994902
2. Antara NS, Gunam IBW, Suhendra L (2024) Evaluation of Paste and Dried Microalgae Biomass and Its Nutritional Value During Storage. *BIO Web of Conferences* 98:06003
3. Arad S (2008) Effect of drying on the biological activities of a red microalgal polysaccharide. *Biotechnology and Bioengineering* 99(2):411–420
4. Arif Y, Singh P, Siddiqui H, Bajguz A, Hayat S (2020) Salinity induced physiological and biochemical changes in plants: An omic approach towards salt stress tolerance. *Plant Physiol Biochem* 156:64–77
5. Arora M, Kaushik A, Rani N, Kaushik CP (2010) Effect of cyanobacterial exopolysaccharides on salt stress alleviation and seed germination. *J Environ Biol* 31(5):701–704
6. Bailliez C, Largeau C, Casadevall E (1986) Immobilization of *Botryococcus braunii* in alginate: influence on chlorophyll content, photosynthetic activity and degeneration during batch cultures. *Applied Microbiology and Biotechnology* 23(5):361–366
7. Banik S, Dutta D (2023) Membrane Proteins in Plant Salinity Stress Perception, Sensing, and Response. *J Membr Biol* 256(2):109–124
8. Benítez SV, Carrasco R, Bucarey B, Noriega F, López-Belchí MD, Hasbún R, Giraldo JD, Schoebitz M (2025) Solid inoculants: Bacterial immobilization routes on the degradation in the soil of alginate-starch-based biofertilizers. *International Journal of Biological Macromolecules* 320(Pt 2):145909
9. Brito-Lopez C, van der Wielen N, Barbosa M, Karlova R (2025) Plant growth–promoting microbes and microalgae-based biostimulants: sustainable strategy for agriculture and abiotic stress resilience. *Philosophical Transactions of the Royal Society B* 380(1927):20240251
10. Castro GM, Tewelde D, Tubaldi E (2025) Assessment of the use of sodium alginate for soil improvement in coastal applications. *Scientific Reports* 15:38714

11. Dey K, Khan RA (2011) Fabrication and Mechanical Characterization of Calcium Alginate Fiber-Reinforced Polyvinyl Alcohol Based Composites. *Polymer-Plastics Technology and Engineering* 50(7):700–706
12. Durairaj M, Ponnusamy R, Ravindran B, Shyu DJH, Thangavel K (2026) Westiellopsis-derived exopolysaccharide: A novel approach to alleviation of salt stress in plants and environmental cleanup. *Algal Research* 93:104458
13. Escalante FME, Cortés-Jiménez D, Tapia-Reyes G, Suárez R (2015) Immobilized microalgae and bacteria improve salt tolerance of tomato seedlings grown hydroponically. *Journal of Applied Phycology* 27(5):1923–1933
14. Heath RL, Packer L (1968) Photoperoxidation in isolated chloroplasts: I. Kinetics and stoichiometry of fatty acid peroxidation. *Archives of Biochemistry and Biophysics* 125(1):189–198
15. Herrera N, Puentes-Escobar TC, Álvarez-Pulido JA, et al. (2025) Effect of microalgae and a cyanobacteria mixture on germinative activity, growth, and cannabinoid production in Cannabis sativa plants. *Journal of Applied Phycology* 37(6):4207–4217
16. Körner T, Zinkernagel J, Röhlen-Schmittgen S (2025) Plant Growth and Metabolic Responses of Tomato Varieties to Salinity Stress After Thermopriming. *Stresses* 5(2):27
17. Li Y S, Sultan H, He A B, Guo X Y, Zhao T C, Khan M N, Ai Z Y, Nie L X (2026) Salt stress in rice: Morpho-physiological effects, nitrogen dynamics and integrated management strategies for yield improvement in saline soils. *Pedosphere* 36(2): 402–415
18. Liang L, Bai X,Hua Z (2022) Enhancement of the immobilization on microalgae protective effects and carbamazepine removal by *Chlorella vulgaris*. *Environmental Science and Pollution Research* 29(52):79567–79578
19. Manimaran, G., Duraisamy, S., Subramanium, T., Rangasamy, A., Alagarsamy, S., James, P., Selvamani, S.B., Perumal, D., Veerappan, M., Arunan, Y.E., & Periakaruppan, J. (2025). Silicon-driven approaches to salinity stress tolerance: Mechanisms, uptake dynamics, and microbial transformations. *Plant Stress* 16(000)
20. Mutale-Joan C, Rachidi F, Mohamed HA, Mernissi NE, Aasfar A, Barakate M, Mohammed D, Sbabou L, El Arroussi H (2021) Microalgae-cyanobacteria–based biostimulant effect on salinity tolerance mechanisms, nutrient uptake, and tomato plant growth under salt stress. *Journal of Applied Phycology* 33(6):3779–3795
21. Nurbekova Z, Satkanov M, Beisekova M, Akbassova A, Ualiyeva R, Cui J F, Chen Y W, Wang Z Q, Zhangazin S (2024) Strategies for Achieving High and Sustainable Plant Productivity in Saline Soil Conditions. *Horticulturae* 10(8): 878
22. Nisha R, Kiran B, Kaushik A, Kaushik CP (2018) Bioremediation of salt affected soils using cyanobacteria in terms of physical structure, nutrient status and microbial activity. *International Journal of Environmental Science and Technology* 15(3):571–580
23. Nogueira JC, dos Santos Gomes Calaça J, Barbosa de Souza Gomes CV, Callou Menezes LE, Inácio Silva JR, Jardim AMRF, Pessoa LGM, Barbosa da Silva JH (2025) Freshwater Algae Biostimulant in

Mitigating Impacts of Saline Irrigation on Onions. *Plants* 14(10):1559

24. Ouzakar S, Skali Senhaji N, Abrini J (2025) Biostimulant effect of Haematococcus pluvialis on the germination of seeds from two Moroccan endemic plants: Origanum compactum and Origanum elongatum. *Journal of Applied Phycology* (2):1075–1088
25. Patel B, Bergi J (2025) Algal Consortia as Green Alternatives: Enhancing Soil Health and Tomato Cultivation. *Asian Journal of Current Research* 10(2):264–272
26. Paul T, Jaiswal P, Govindasamy V, Pandey R, Kumar S, Abraham G (2026) Cyanobacterial seed priming and inoculation mitigates salinity stress in transplanted rice through the regulation of growth, photosynthesis and ion metabolism. *Journal of Applied Phycology*
27. Priya S, Burns M B, Ward T L, Mars R A, Adamowicz B, Lock E F, Kashyap P C, Knights D, Blekhman R (2022). Identification of shared and disease-specific host gene–microbiome associations across human diseases using multi-omic integration. *Nature Microbiology* 7:780–795
28. Rippka R, Deruelles J, Waterbury J B, Herdman M, Stanier R Y (1979). Generic assignments, strain histories and properties of pure cultures of cyanobacteria. *J.gen.microbiol* 111(1):2506.
29. Sarhan N, Arafa EG, Elgedawy N, Elsayed KNM, Mohamed F (2024) Urea intercalated encapsulated microalgae composite hydrogels for slow-release fertilizers. *Scientific Reports* 14:15032
30. Sarsekeyeva FK, Sadvakasova AK, Sandybayeva SK, Kossalbayev BD, Huang ZY, Zayadan BK, Akmukhanova NR, Leong YK, Chang JS, Allakhverdiev SI (2024) Microalgae- and cyanobacteria-derived phytostimulants for mitigation of salt stress and improved agriculture. *Algal Research* 82:103686
31. Senousy HH, Hamoud YA, Abu-Elsaoud AM, Al Zoubi OM, Abdelbaky NF, Zia-ur-Rehman M, Usman M, Soliman MH (2023) Algal Bio-Stimulants Enhance Salt Tolerance in Common Bean: Dissecting Morphological, Physiological, and Genetic Mechanisms for Stress Adaptation. *Plants* 12(21):3714
32. Spitz DR, Oberley LW (1989) An assay for superoxide dismutase activity in mammalian tissue homogenates. *Analytical Biochemistry* 179(1):8–18
33. Stirk WA, Bálint P, Vambe M, Kulkarni MG, van Staden J, Ördög V (2021) Effect of storage on plant biostimulant and bioactive properties of freeze-dried *Chlorella vulgaris* biomass. *Journal of Applied Phycology* 33(6):3797–3806
34. Sun ZL, Liu XY, Ugya AY, Liu HY, Sun LQ, Luo GL (2026) Microalgae and cyanobacteria as a tool for agricultural sustainability: a review of biofertilizer and biostimulant potential. *Frontiers in Plant Science* 16:1733394
35. Szabados L, Kant K, Rabilu S, Rashid A, Zsigmond L (2026) Crops exposed to extreme conditions: perspectives of gene editing to improve stress tolerance. *Plant Cell Reports* 45:207
36. Tang H, Du L, Xia C, Luo J (2024) Bridging gaps and seeding futures: A synthesis of soil salinization and the role of plant-soil interactions under climate change. *iScience* 27(9):110804
37. Wang T, Li D, Tian X, Huang GL, He ML, Wang CH, Kumbhar AN, Woldemicael AG (2024) Mitigating salinity stress through interactions between microalgae and different forms (free-living & alginate

gel-encapsulated) of bacteria isolated from estuarine environments. *Science of the Total Environment* 927:172327

38. Yuan J, Cao H, Qin W, Yang S, Zhang D, Zhu L, Song H, Zhang Q (2025) Genomic and modern biotechnological strategies for enhancing salt tolerance in crops. *New Crops* 2:100057
39. Zhang Y, Ding S, Xue X, Hu X, Rehman OU, Liu W, Zhu F, Wang R, Sobhi M, Wang F, Huo S (2025) Combined application of nitrogen-fixing cyanobacteria enhances rice growth and nutritional quality in saline environments. *Algal Research* 89:104061

Figures



Figure 1

Morphology of the three *C. vulgaris* biostimulants formulations used in this study. APo: oven-dried algal powder prepared at 80°C for 10 hours; APa: algal paste obtained by centrifugation of freshly harvested algal biomass; IABs: immobilized algal beads fabricated by entrapping fresh algal paste in SA–PVA gel beads cross-linked with $CaCl_2$. Scale bar = 1 cm.



Figure 2

Morphology of *O. sativa* L. cv. White Awn seedlings under different treatments after 14 days of salt stress. CK: without NaCl or microalgal biofertilizer; T0:50 mM NaCl stress only; T1: 50 mM NaCl + 1 g·L^{-1} algal powder; T2: 50 mM NaCl + 1 g·L^{-1} algae paste; T3: 50 mM NaCl + 1 g·L^{-1} immobilized algal beads. Scale bar = 5 cm.

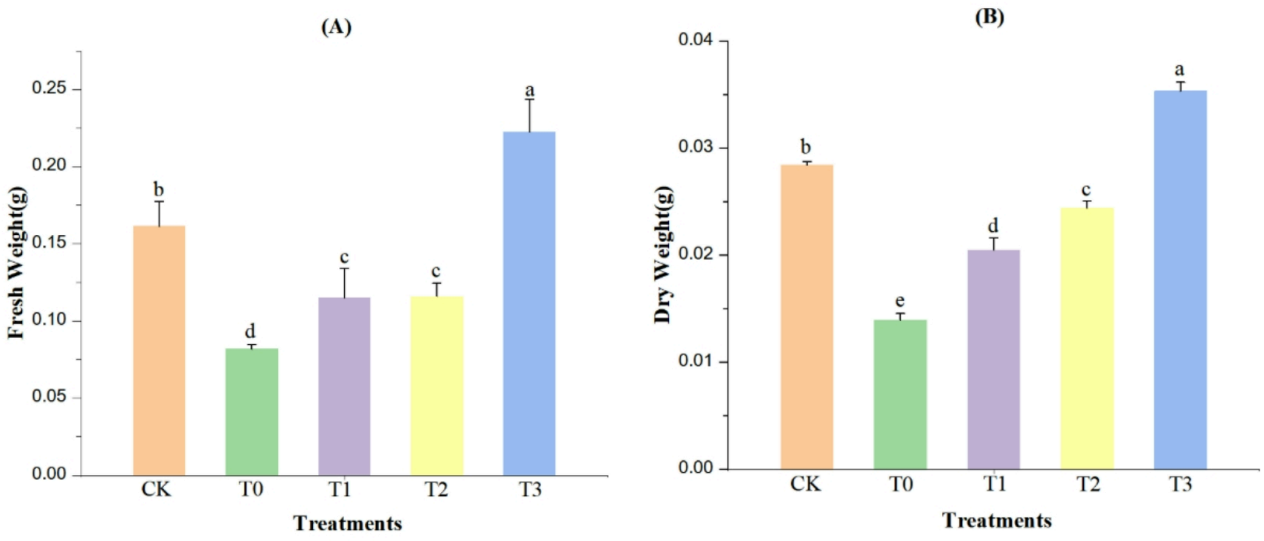


Figure 3

FW (A) and DW (B) of *O. sativa* L. cv. White awn under different treatments after 14 days of salt stress. CK: distilled water without NaCl; T0: 50 mM NaCl stress only; T1: 50 mM NaCl + 1 g·L⁻¹ algae powder; T2: 50 mM NaCl + 1 g·L⁻¹ algae paste; T3: 50 mM NaCl + 1 g·L⁻¹ immobilized algal beads. Values are presented as mean ± standard error (n = 3). Different lowercase letters above the bars indicate significant differences among treatments at $P < 0.05$ (Duncan's multiple range test).

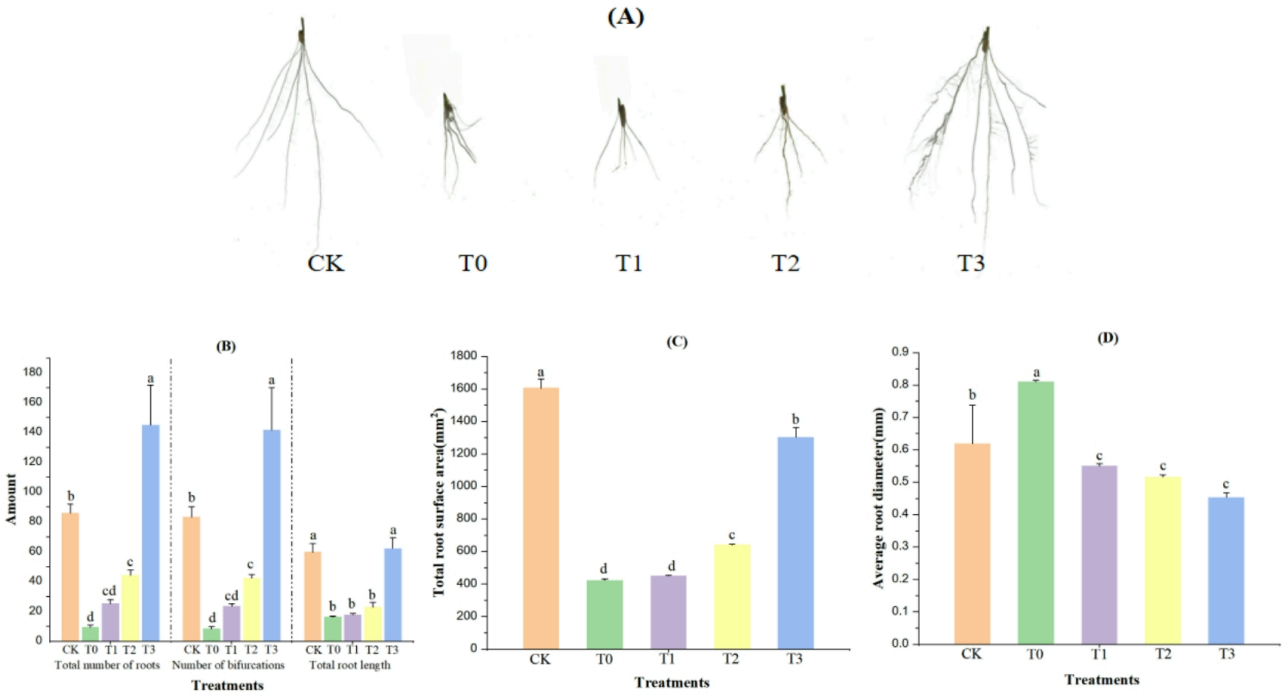


Figure 4

Root scanning images of *O. sativa* L. cv. White Awn seedlings under different treatments after 14 days of salt stress (A). Total number of root tips, total root length, and number of biofurcations (B).Total root surface area (C). Average root diameter (D). CK: distilled water; T0: 50 mM NaCl stress only; T1: 50 mM NaCl + 1 g·L⁻¹ algae powder; T2: 50 mM NaCl + 1 g·L⁻¹ algae paste; T3:50 mM NaCl + 1 g·L⁻¹ immobilized algal beads. Root images were acquired using a root scanning system (WinRHIZO). Scale bar = 2 cm.

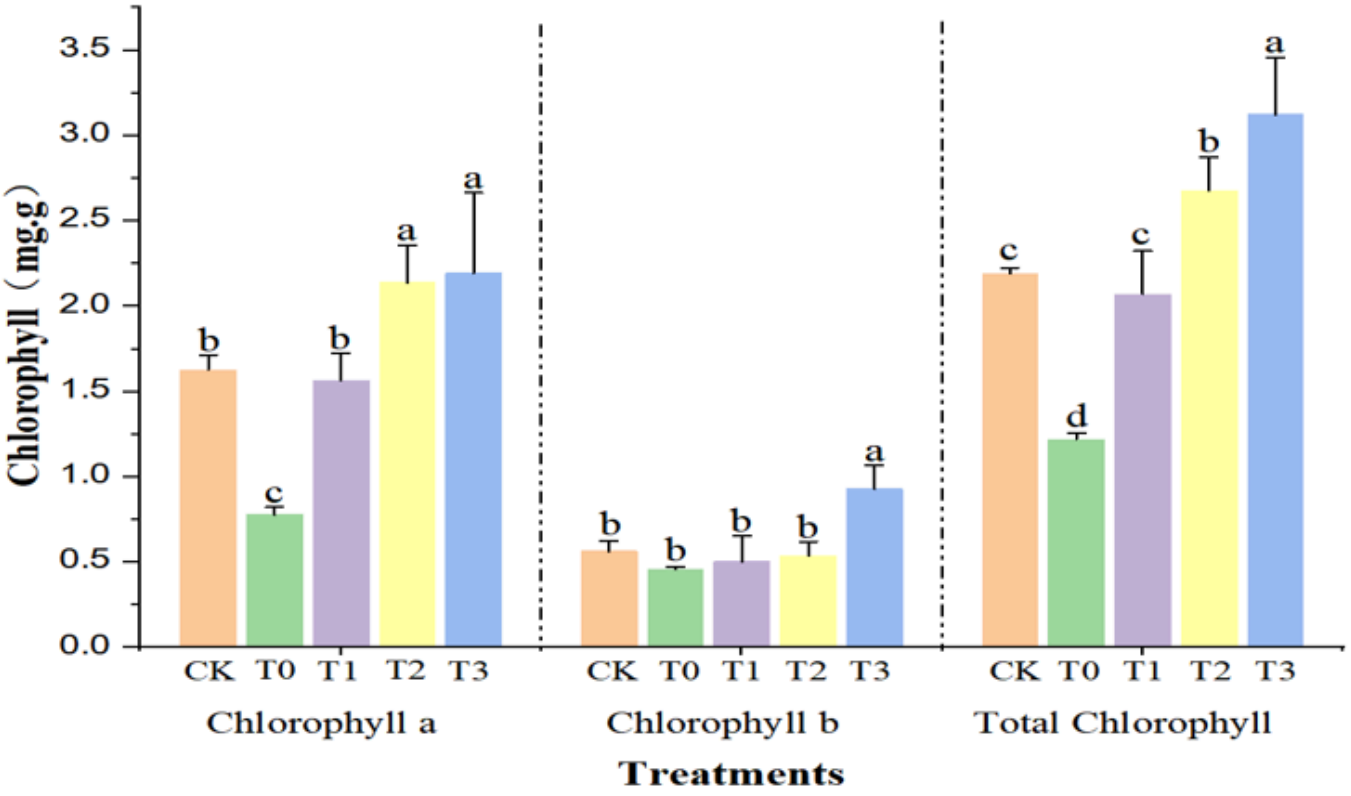


Figure 5

Chlorophyll a, chlorophyll b, and total chlorophyll contents in the leaves of *O. sativa* L. cv. White Awn seedlings under different treatments after 14 days of salt stress. CK: distilled water without NaCl; T0: 50 mM NaCl stress only; T1: 50 mM NaCl + 1 g·L⁻¹ algae powder; T2: 50 mM NaCl + 1 g·L⁻¹ algae paste; T3: 50 mM NaCl + 1 g·L⁻¹ immobilized algal beads. Chlorophyll content was determined using acetone–ethanol extraction. Values are presented as mean ± standard error (n = 3). Different lowercase letters above the bars indicate significant differences among treatments at $P < 0.05$ (Duncan's multiple range test).

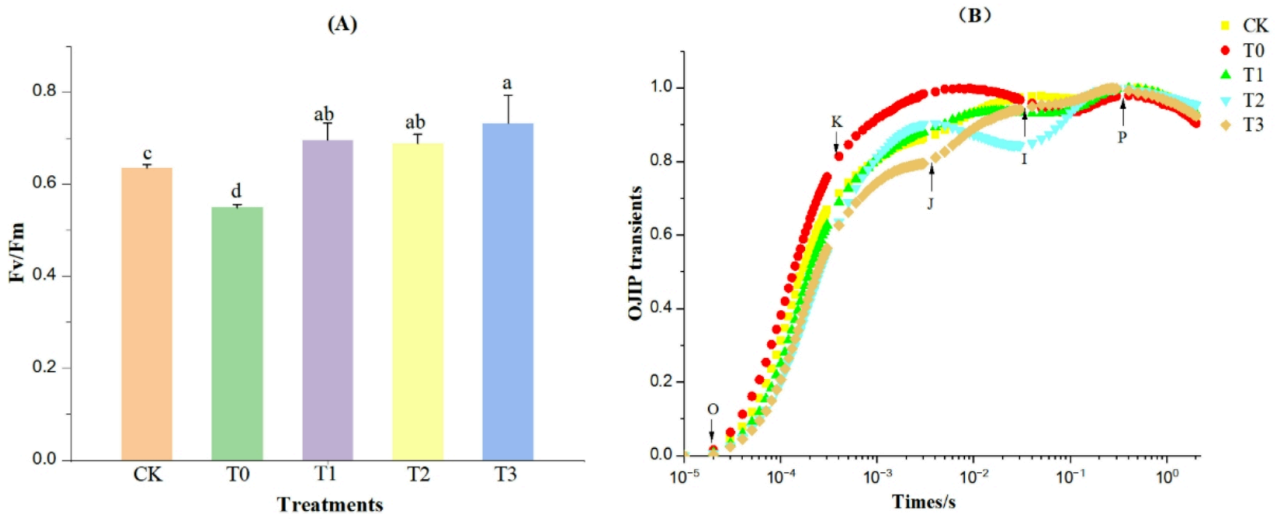


Figure 6

Chlorophyll fluorescence parameters of *O. sativa* L. cv. White Awn, different treatments after 14 days of salt stress. (A) Maximum photochemical efficiency of PSII (Fv/Fm); (B) OJIP fluorescence induction transients. CK: distilled water without NaCl; T0: 50 mM NaCl stress only; T1: 50 mM NaCl + 1 g·L⁻¹ algae powder; T2: 50 mM NaCl + 1 g·L⁻¹ algae paste; T3: 50 mM NaCl + 1 g·L⁻¹ immobilized algal beads. Fv/Fm was measured after 20 minutes of dark adaptation using a portable chlorophyll fluorometer. OJIP transients were recorded under saturating red light at 3000 μmol·m⁻²·s⁻¹. Values in (A) are presented as mean ± standard error (n = 3). Different lowercase letters above the bars indicate significant differences among treatments at $P < 0.05$ (Duncan's multiple range test).

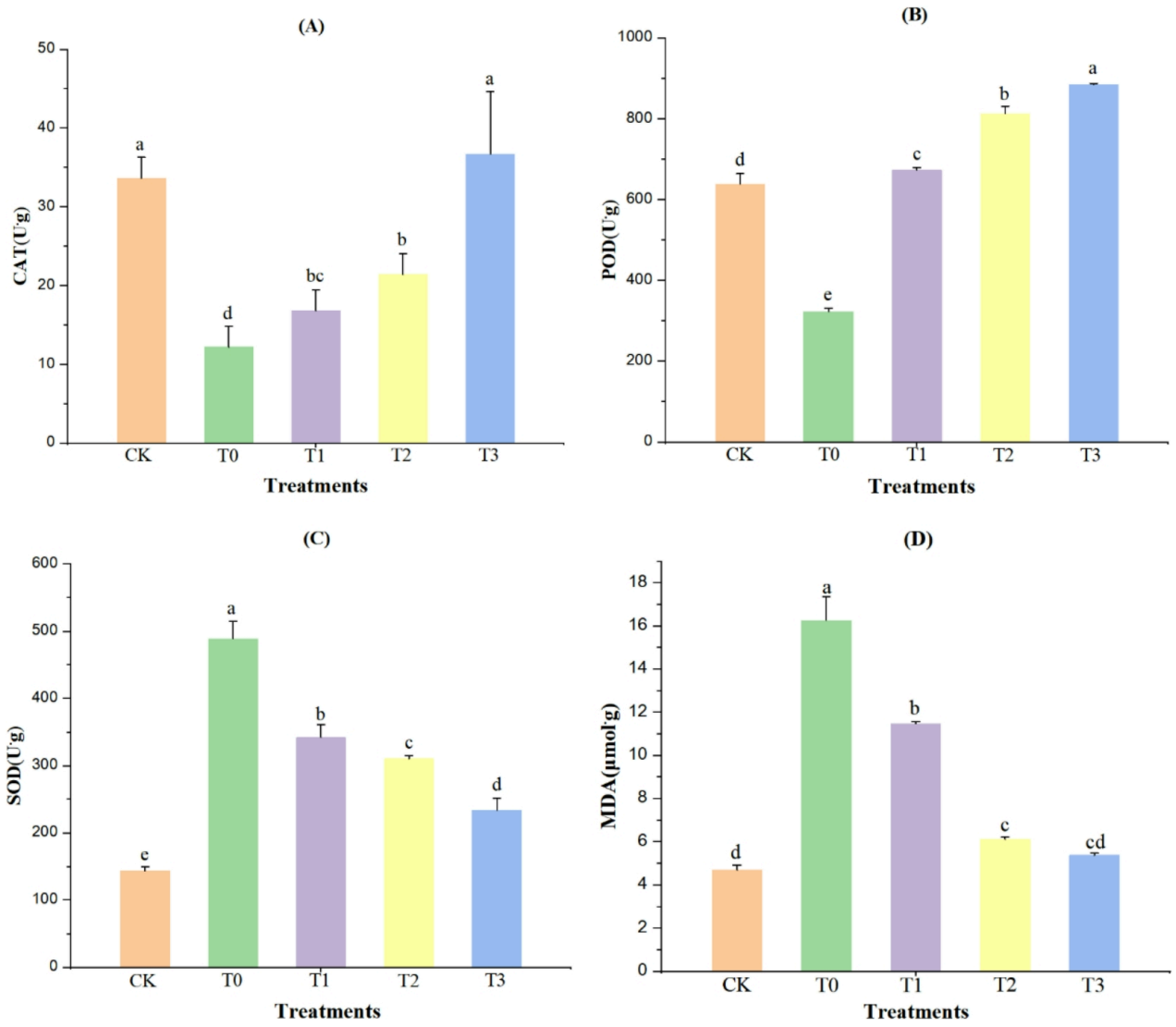


Figure 7

Antioxidant enzyme activity and MDA content in the leaves of *O. sativa* L. cv. White Awn. different treatments after 14 days of salt stress. (A) CAT activity; (B) POD activity; (C) SOD activity; (D) MDA content. CK: distilled waterwithout NaCl; T0: 50 mM NaCl stress only; T1: 50 mM NaCl + 1 g·L⁻¹ algae powder; T2: 50 mM NaCl + 1 g·L⁻¹ algae paste; T3: 50 mM NaCl + 1 g·L⁻¹ immobilized algal beads. Enzyme activity and MDA content were determined using commercial assay kits, following the manufacturer's protocols. Values are presented as mean ± standard error (n = 3). Different lowercase letters above the bars indicate significant differences among treatments at $P < 0.05$ (Duncan's multiple range test).